Binary and Ternary Blends of Polyethylene, Polypropylene, and Polyamide 6,6: The Effect of Compatibilization on the Morphology and Rheology

R. Krache,[1] D. Benachour,[1] P. Pötschke[2]

[1]*Laboratory of Multiphase Polymeric Materials, Faculty of Engineering, Ferhat Abbas University, Setif, Algeria*
[2]*Institute of Polymer Research, Hohe Strasse 6, D-01069, Dresden, Germany*

Received 1 October 2003; accepted 5 May 2004
DOI 10.1002/app.21098
Published online in Wiley InterScience (www.interscience.wiley.com).

ABSTRACT: The effects of two compatibilizing agents, polystyrene–poly(ethylene butylene)–polystyrene copolymer (SEBS) and SEBS-grafted maleic anhydride (SEBS-*g*-MAH), on the morphology of binary and ternary blends of polyethylene, polypropylene, and polyamide 6,6 were investigated with scanning electron microscopy and melt rheology measurements. The addition of the compatibilizers led to finer dispersions of the particles of the minor component and a decrease in their size; this induced a significant change in the blend morphology. The rheological measurements confirmed the increased interaction between the blend components, especially with SEBS-*g*-MAH as the compatibilizer. New covalent bonds could be expected to form through an amine–anhydride reaction. © 2004 Wiley Periodicals, Inc. J Appl Polym Sci 94: 1976–1985, 2004

Key words: blends; morphology; polyamides; polyethylene (PE); poly(propylene) (PP); rheology

INTRODUCTION

Most studies on polymer blends deal with binary systems, and the objective is to obtain desirable properties,[1–5] For this purpose, compatibilizing agents are often used. Such agents are added to enhance the compatibility of two immiscible blend components by reducing the interfacial tension to obtain finer dispersions and enhanced phase adhesion and, at the same time, to improve the processing stability of blends by reducing coalescence effects.[6–8] In the pursuit of new polymeric blend materials, attention has also been drawn to systems with more than two phases. More recently, ternary systems have been receiving more attention, despite the difficulties encountered during the study of such materials. The main attraction of this type of blend resides in the multiple types of phase morphology that can be obtained and their direct influence on the whole set of properties, starting with the rheological behavior during processing.[9–11]

The basic material parameters affecting flow-induced blend morphology are the blend composition, viscosity ratio, and melt elasticity ratio during blending conditions, as well as the interfacial tension.[12–19] Different morphology types can be obtained, and they are divided into four major categories: dispersed particle–matrix structures, matrix–fiber structures, lamellar structures, and cocontinuous structures.[14,20] In blends consisting of three or more phases, quite different mixed morphologies can be obtained, and they depend mainly on the composition ratio and the interfacial tension between the components as well as the viscosity relationships between the different components under the processing conditions. The compatibilizing agent can have a large impact on the morphology of a polymer blend because it can change the morphology type and the phase dimensions by lowering the interfacial tension and changing the interfacial or component viscosities. In most cases, the added compatibilizer contains segments that are capable of specific interactions or chemical reactions with the blend components; in the latter case, block or graft copolymer can be generated *in situ*, close to the interface, during the blend mixing, which has been shown to be much more effective.

In a recent article,[21] Jafari et al. reported data on multicomponent blends based on polyamide 6 (PA6) and styrenic polymers. For PA6/SAN (styrene–acrylonitrile copolymer) blends, a dispersed morphology changed into a cocontinuous structure after a reactive compatibilizer was added; for PA6/ABS (acrylonitrile–butadiene–styrene terpolymer) blends, the addition of the reactive compatibilizer refined the cocontinuous structure and increased the viscosity and elasticity of the system.

Much research has been done in the field of binary thermoplastic polymer blends, but few studies have dealt with the combination of the characteristics of

Correspondence to: R. Krache (rachida2000fr@yahoo.fr).

TABLE I
Blend Compositions, Compatibilizers, and Some Rheological Characteristics of the Components and Blends

PP/PE/PA (w/w/w)	Compatibilizer type (wt %)	Activation energy (kJ/mol)	Viscosity (Pa s) at 100 rad/s and 270°C	Zero shear viscosity (Pa s)		
				190°C	230°C	270°C
100/0/0	—	39[a]	188	2600	1258	664
0/100/0	—	28[b]	250	1032	887	651
0/0/100	—	—	187	—	—	2158
50/50/0	—	33[a]	205	2000	1084	649
50/50/0	10N2	44[a]	202	N/A	N/A	N/A
50/0/50	—	—	95	—	—	7572
50/0/50	15N1	—	147	—	—	N/A
0/50/50	—	—	177	—	—	5112
0/50/50	15N1	—	361	—	—	N/A
33/33/33	—	—	141	—	—	4412
33/33/33	15N1	—	266	—	—	N/A

N/A, Ellis and Carreau models were not applicable; N1 = SEBS-g-MAH; N2 = SEBS.
[a] Calculated from values at 190, 230, and 270°C.
[b] Calculated from values at 230 and 270°C.

three major polymers, such as polypropylene (PP), polyethylene (PE), and polyamide (PA), despite the commercial importance of these three polymers.[22–25] The aim of this work is to compare ternary blends of PE, PP, and polyamide 6,6 (PA6,6) from morphological and rheological points of view and to investigate the effect of two compatibilizing agents, a polystyrene–poly(ethylene butylene)–polystyrene copolymer (SEBS) and SEBS-grafted maleic anhydride (SEBS-*g*-MAH), on these behaviors. In addition, binary blends of the three polymers have been studied for comparison.

EXPERIMENTAL

Materials

PP (Vestolen P5000, Chemische Werke Hüls, AG, Marl (Germany)), high-density PE (Lupolen 6031M, BASF GmbH, Munchsmunster (Germany)), and PA6,6 (Duretane A30, Bayer AG, (Germany)) were used. The densities of PP, PE, and PA were 0.902, 0.963, and 1.140 g/cm^{3,} respectively.

The compatibilizers were two triblock thermoplastic elastomers from Shell: Kraton G1652 and Kraton FG 1901X (Houston, TX, USA). Kraton G1652 (SEBS) has polystyrene end blocks with a molecular weight of 7200 g/mol and a midblock of PE of poly(ethylene-*co*-butylene) (EB) with a molecular weight of 37,500 g/mol; its density is 0.90 g/cm^3, and it is known to be a good compatibilizer for polyolefinic blends. Kraton FG 1901X (SEBS-*g*-MAH) is essentially a low-molecular-weight SEBS copolymer grafted with 2 wt % maleic anhydride (MAH); its density is 0.919 g/cm^3, and its polymeric styrene content is 28 wt %. The glass-transition temperature of the rubber phase is −42°C, and it is a very convenient compatibilizer for blends containing PA. Before the processing and rheological measurements, PA and blends containing PA were dried for a period of 16 h at 65°C to remove absorbed water.

Blend preparation

All blends were prepared via melt mixing with a Haake corotating twin-screw extruder (Karlsruhe, Germany) with a length/diameter ratio of 40. The screw speed was set to 140 rpm, and except for the feed zone, the barrel setting temperature was 270°C for all blends containing PA and 230°C for the other polyolefinic blends. The residence time was about 2 min. The hot extrudates were immediately quenched in water and pelletized.

The blend compositions, based on weight percentages, are presented in Table I.

The test samples were prepared in the form of 100-mm-long tensile bars (cross section = 6 mm × 4 mm) with an Arburg 270S injection-molding machine (Losburg, Germany). The melt and mold temperature were 270 and 70°C, respectively, for the PA and blends containing PA and 250 and 60°C for the polyolefins and their blends.

Methods

Melt rheology measurements were performed with an Advanced Rheometric Expansion System (ARES) rheometer (Rheometrics, Inc., Piscataway, NJ, USA) in a parallel-plate geometry, in an oscillation mode, on properly dried pellets of the extruded blend components. Frequency sweeps in the range of 0.1–100 rad/s were performed at 270°C for PA and its blends and at 230°C for the polyolefinic blends in an atmosphere of N_2. A strain of 5% was used, which was determined to be within the linear viscoelastic range. Sweeps with

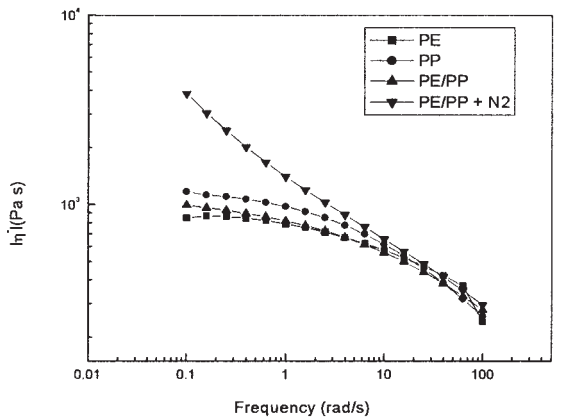

Figure 1 Complex viscosity of PE/PP blends at 230°C.

increasing and decreasing frequency were performed to check the stability of the blends; for interpretation, the sweep with decreasing frequency was used. With ARES software, the zero-shear viscosities were calculated with the Ellis or Carreau model.

Morphological characterization was performed with scanning electron microscopy (SEM). Injection-molded specimens were broken cryogenically in liquid nitrogen. In addition, smooth surfaces were prepared with a rotational microtome (Jung RM2055, Leica, Wetzlar, Germany) equipped with a steel knife at a temperature lower than −60°C. In blends containing PA as the dispersed phase, selective etching of the cut surface was performed by the samples being hung at a depth of about 1–3 mm into formic acid (98%) for a period of about 4 h. The etching procedure was applicable only for blends in which PA was supposed to form a dispersed phase; this was checked by the immersion of pieces of granules and injection-molded samples into formic acid for a period longer than 1 day. After being sputter-coated with a thin film of gold, the specimens were examined in a 435 VP scanning electron microscope (Leo Elektronenmikroskopie, GmbH, Oberkochen, Germany).

RESULTS AND DISCUSSIONS

Rheological study

PP/PE binary blends

Figure 1 compares the complex viscosity versus the frequency for PP/PE (50/50) blends, with and without SEBS, along with that of the components, at 230°C. The viscosity of PE was lower than that of PP over the whole frequency range. The extrapolated zero-shear viscosities (measured at three temperatures) are shown in Table I. At the melt blending temperature of 230°C, the viscosity values of the noncompatibilized blend lay between those of the homopolymers.

To estimate which phase formed the matrix by predicting the phase-inversion composition, we used Paul's model,[13,26] which equals the phase-inversion volume ratio with the viscosity ratio between the blend components under the processing conditions. It was assumed that the mean shear rate in the extrusion process was about 100 s^{-1}. Assuming the validity of the Cox–Merz rule in relating the steady-shear viscosity with the absolute value of the complex viscosity,[27] we used the viscosity values measured in frequency sweeps at 100 rad/s to calculate the viscosity ratio. The predicted phase-inversion compositions for the binary blends are given in Table II. According to this, PE should form the matrix in binary 50/50 blends. The viscosity curve of the blend also supported this finding because the blend viscosity, which was always mainly determined by the matrix viscosity, was more similar to that of PE than to that of PP.

The addition of SEBS led to a significant increase in the complex viscosity, especially at low frequencies, and this was probably due to the elastomeric nature of SEBS. The viscosity increased linearly as the frequency decreased and thus did not show a Newtonian plateau at low frequencies. Therefore, no zero-shear viscosity is given in Table I. The compatibility was expected to be achieved through the affinity of the middle block (EB) of SEBS toward the two homopolymers.

The storage modulus (G') of the compatibilized PP/PE (50/50) blends is plotted against the frequency in Figure 2. The compatibilized blends showed higher G' values than the uncompatibilized blend over the entire range of frequencies. As shown, the compatibilizer SEBS could result in a great difference in the rheological properties (complex viscosity and G'). From these results, we concluded that the presence of SEBS led to a lowering of the interfacial tension and an increase in the adhesion between the individual phases.

TABLE II
Phase Inversion Prediction According to Paul and Barlow[13] for the Investigated Binary Blends

	Volume ratio (ϕ_2/ϕ_1) and viscosity ratio (η_1/η_2)					
	ϕ_{PP}/ϕ_{PE}	η_{PE}/η_{PP}	ϕ_{PA}/ϕ_{PE}	η_{PE}/η_{PA}	ϕ_{PA}/ϕ_{PP}	η_{PP}/η_{PA}
	1.06	1.45	0.84	1.33	0.8	1
	1.53 (>1)		1.11 (>1)		0.8 (<1)	
$\eta_1/\eta_2 \times \phi_2/\phi_1$	PE matrix		PE matrix		PA matrix	

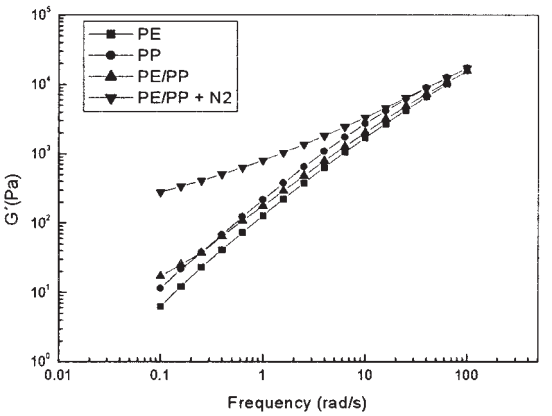

Figure 2 G' of PE/PP blends at 230°C.

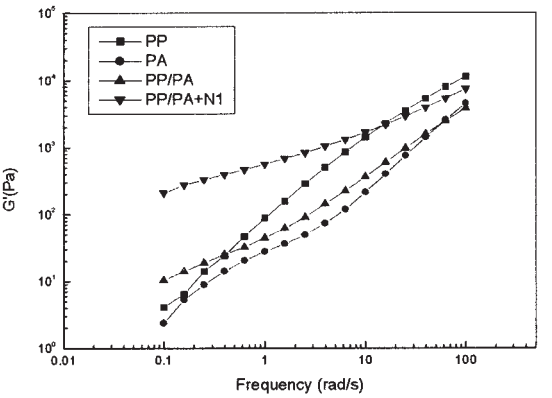

Figure 4 G' of PP/PA blends at 270°C.

PP/PA binary blend at 270°C

Figure 3 shows the changes in the complex viscosity with the frequency of a binary blend of PP and PA (50/50) with and without compatibilizer SEBS-*g*-MAH. Both PP and PA exhibited Newtonian behavior, and the viscosity of PP was higher than that of PA; for their blend (50/50), the plot of the dynamic viscosity (η^*) versus the frequency was under those of their homologous polymers. The monotonous increase in the viscosity with the frequency may be related to the lack of adhesion between the two incompatible polymers. With the addition of the compatibilizer, the blend viscosity increased rapidly over the entire frequency range, but it remained lower than that of PP at a higher frequency. This increase was probably due to an enhancement in the interfacial interaction between the two polymers, which was associated with the grafting reaction between MAH and the amino end groups of PA and with the elastomeric nature of the compatibilizer. G' of the compatibilized PP/PA blends is plotted against the frequency in Figure 4. The compatibilized blend showed a higher G' value than the uncompatibilized blend for all frequencies. As shown in Figures 3 and 4, the compatibilizer SEBS-*g*-MAH could induce large differences in the rheological properties. G' of PP was also higher than that of pure PA and their uncompatibilized PP/PA blend.

PE/PA binary blend at 270°C

Figure 5 illustrates the variation of the complex viscosity with the frequency for the investigated PA/PE blends. The disposition of the curve for the uncompatibilized blend is situated between those of PE and PA. Both homopolymers exhibited a Newtonian plateau, and the viscosity of PA was lower than that of PE. The addition of the SEBS-*g*-MAH compatibilizer led to an increase in the viscosity with decreasing frequency; this demonstrated a viscoelastic behavior that could be explained by the rubbery nature of the compatibilizer and probably the grafting reaction that took place between MAH and the amino end groups of PA6,6 [it was also observed that the values of G' were lower that the values of the loss modulus (G'') for PA, PE, and PA/PE without the compatibilizer, but for the compatibilized blend, the values of G' exceeded those of G''; this is also an indication of the homogeneity of the system; see Fig. 6].

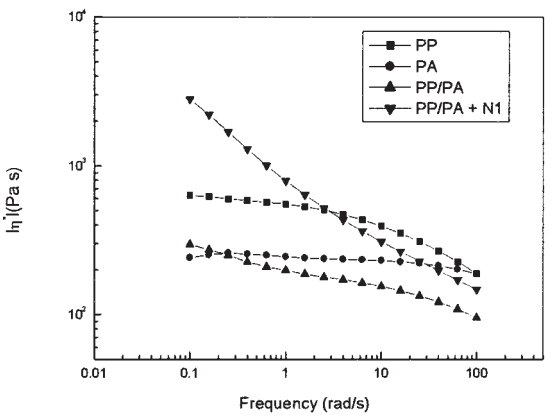

Figure 3 Complex viscosity of PP/PA blends at 270°C.

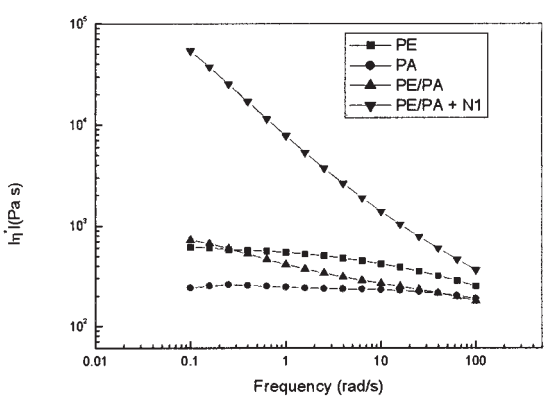

Figure 5 Complex viscosity of PE/PA blends at 270°C.

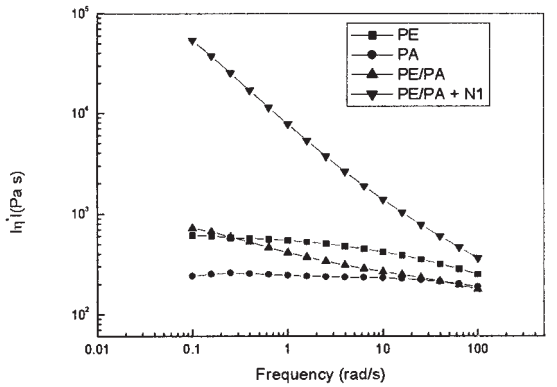

Figure 6 G' of PE/PA blends at 270°C.

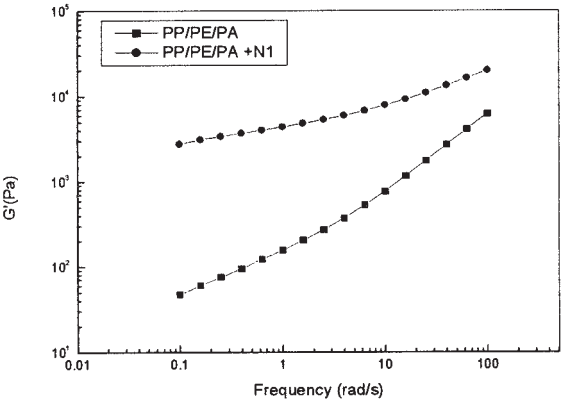

Figure 8 G' of PP/PE/PA blends at 270°C.

PP/PE/PA ternary blend at 270°C

The complex viscosity of the ternary system PP/PE/PA (Fig. 7) showed a small increase as the frequency decreased. The combination of the three polymers id not present Newtonian behavior. With the addition of the compatibilizer (SEBS-*g*-MAH), a large and linear increase in η^* was obtained over the entire frequency range, and the difference between the compatibilized and uncompatibilized blends was more pronounced at lower frequencies. The compatibilized system behaved as a viscoelastic one. Figure 8 illustrates the variation of G' with the frequency. The presence of the compatibilizer in the blend led to a remarkable increase in G', an increase that was more pronounced at lower frequencies. In general, G' increased with the frequency.

G' versus G''

The contribution of the viscous component to the viscoelastic behavior is given by G'' or η^*, whereas the elastic behavior is represented by G'. Plots of log G' versus log G'' illustrate the relative contribution of the G'' response to that of G'. This mode of presentation was suggested by Han[21] because it was found to be independent of the temperature and molecular weight for monodisperse materials and very sensitive to the molecular weight distribution and to short-chain and long-chain branching.

The increase in G' could be attributed to the entanglements in the compatibilized blend, as demonstrated by Han[21] and coworkers for polyolefinic blends. Certain rheological parameters such as G', G'', and η^* could be used to determine compatibility. The change in the microstructure of the blends and the compatibility of the polymers could also be predicted from the variation of G' versus G'' of the polymers.

Figures 9–12 show the relationships between G' and G''. The slopes of these graphs for the homopolymers and the blends without the compatibilizer are almost the same, although those of the compatibilized blends are totally different.

At a low frequency, we can say that the structure of the compatibilized blends changed with respect to that of the uncompatibilized blends. The elasticity increased because of yield stress, and a cocontinuous structure was developed.

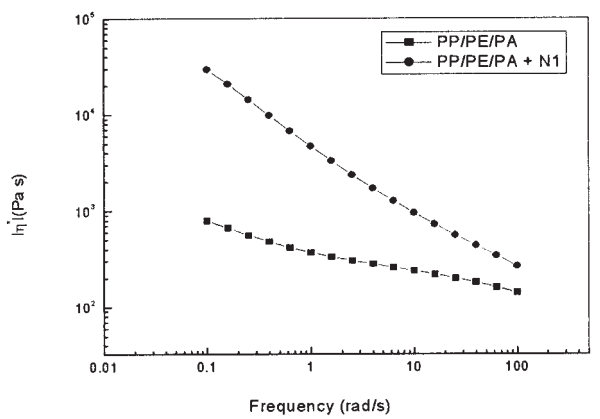

Figure 7 Complex viscosity of PP/PE/PA blends at 270°C.

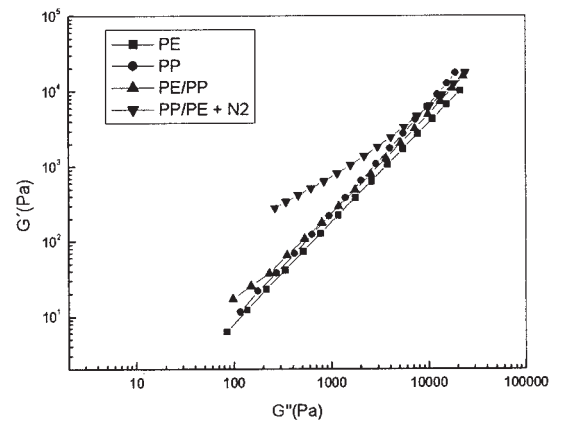

Figure 9 G' as a function of G'' of PP/PE blends at 230°C.

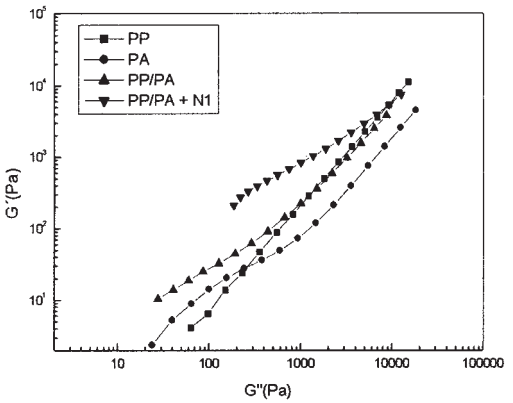

Figure 10 G' as a function of G'' of PP/PA blends at 270°C.

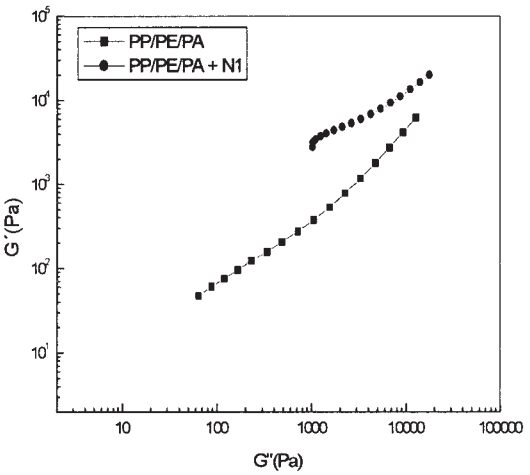

Figure 12 G' as a function of G'' of PP/PE/PA blends at 270°C.

Remarks

From our observations of the dissolution behavior of the different samples in formic acid (except for the polyolefinic blends), a good solvent for PA, we concluded that most of the samples conserved their shape. This meant that PA was not the matrix, except for the PA/PP (50/50) blend, for which we observed the dissolution of part of the sample with the formation of fibrils.

From Paul's equations,[13] we concluded that PA was the matrix for the PP/PA (50/50) blend; PE was the matrix for the PP/PE (50/50) blend and PE/PA (50/50) blend (see Table II).

Morphological observations

PP/PE binary blend

Figures 13(a,b) represent SEM micrographs of the cryofractured surface of injection-molded samples of PP/PE (50/50) blends with and without compatibilizer SEBS, respectively. The contrast of the phases was not good enough to distinguish between the existing two phases in the system without the compatibilizer. According to the rheological measurements, the continuous phase consisted of PE, and the dispersed one consisted of PP. The addition of the compatibilizer SEBS to PP/PE led to a significant change in the morphology; we could observe that the dispersion of the minor phase was finer, and the system became more homogeneous in comparison with that without SEBS.

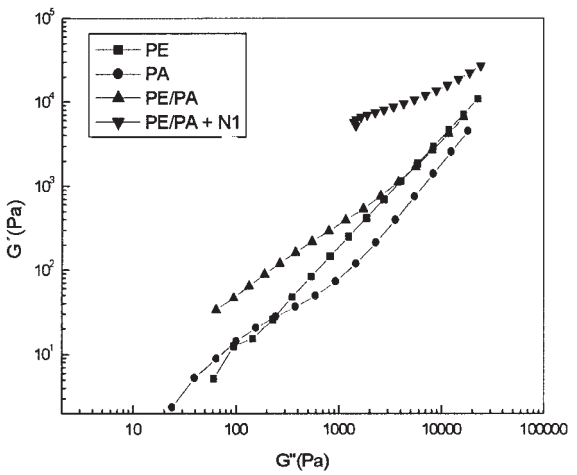

Figure 11 G' as a function of G'' of PE/PA blends at 270°C.

PP/PA binary blend

The SEM images [Fig. 14(a)] clearly show two separate phases, a continuous one forming the matrix (represented by PA), and a dispersed phase (represented by PP). The materials deform by voiding and second-phase particle debonding, as noted on the cryofractured surfaces. The dispersed-phase domains represent a cross section through a mixture of elongated (with a length/diameter ratio of up to ca. 80/30) large-volume domains and small-volume phase domains of near spherical shape (varying from 2 to 20 μm in diameter).

Figure 14(b) illustrates morphological observations of the PP/PA binary blend with 15% SEBS-*g*-MAH. In the micrographs, the transition from the dispersed structure to the cocontinuous structure with very small particles dispersed on the surface can be observed. These particles may be associated with those of the nonreactive compatibilizer. The fine dispersion of the minor phase in the presence of the compatibilizer is also confirmed by the reduction of the diameter of the PA particles, as revealed by the micrographs of the etched surface of the compatibilized system [see Fig. 14(c)]. The cocontinuous structure can be clearly observed, and the dark regions represent the extracted

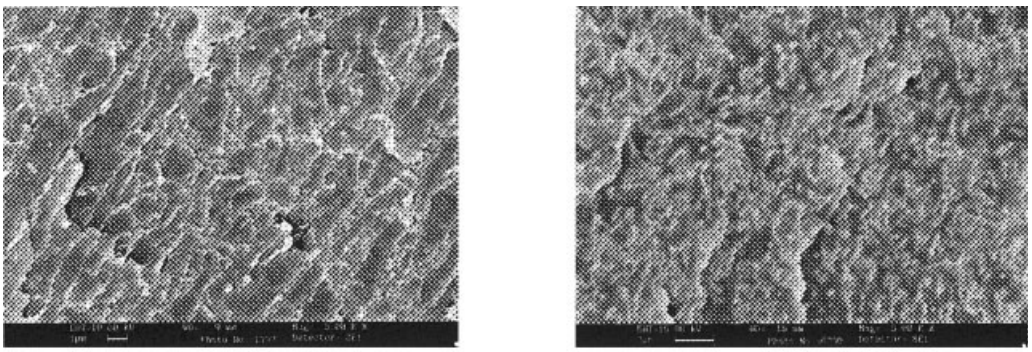

Figure 13 SEM micrographs of the cryofractured surface of PE/PP blend samples (a) without and (b) with compatibilizer SEBS.

PA domains (2–0.5 μm). The cocontinuous structure was also confirmed by rheology, through the increase in the complex viscosity with decreasing frequency (which indicated the presence of the yield stress with the compatibilizer, responsible for the improvement in the interfacial adhesion between the individual phases and the diminution of coalescence).

PE/PA binary blend

Figure 15(a) presents morphological observations of the cryofractured and etched surfaces of the PE/PA binary blend without the compatibilizer. The micrograph shows that PA, forming the discontinuous phase, was present as microvoid domains of a spherical shape of about 2–4 μm and also as vertical and horizontal batons (strips) 50–75 μm long. PE formed the continuous phase as spherical domains of about 20 μm in diameter and with inclusions of PA. We concluded that this blend represented separate phases caused by a lack of adhesion between the two polymers. The etched surface of this system [Fig. 15(b)] also confirmed the dispersion of PA particles with spherical domains of 5–1 μm.

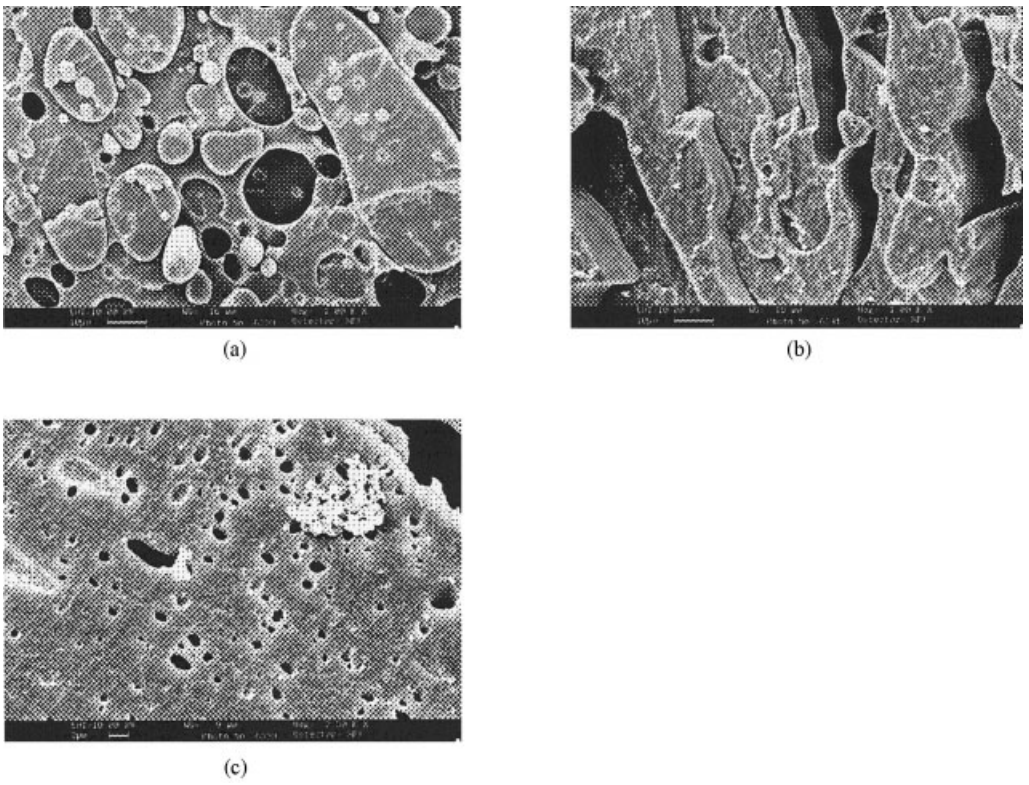

Figure 14 SEM micrographs of (a,b) the cryofractured surface of PP/PA blend samples without and with compatibilizer SEBS-*g*-MAH, respectively, and (c) the etched surface of PP/PA blend samples with compatibilizer SEBS-*g*-MAH.

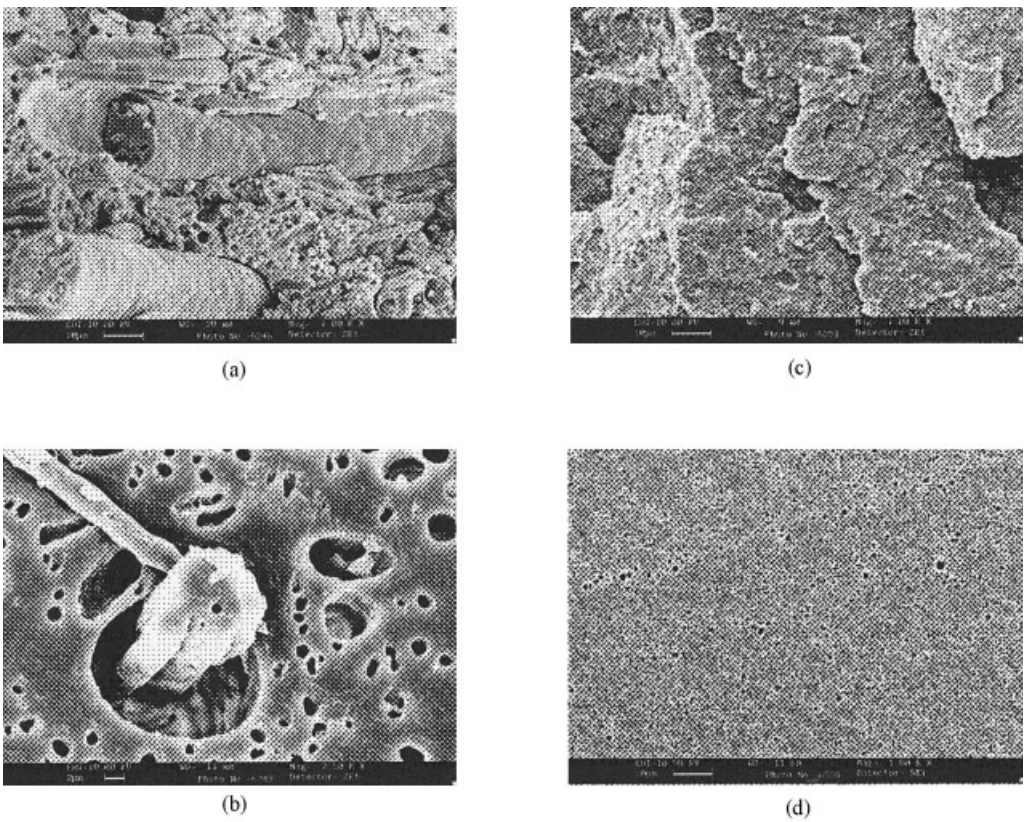

Figure 15 SEM micrographs of (a,c) the cryofractured surface of PE/PA blend samples without and with compatibilizer SEBS-*g*-MAH, respectively, and (b,d) the etched surface of PE/PA blend samples without and with compatibilizer SEBS-*g*-MAH, respectively.

The addition of SEBS-*g*-MAH as a compatibilizer resulted in a remarkable change in the morphology of the PE/PA blend, as revealed by the microscopy image of the cryofractured surface [Fig. 15(c)], and a cocontinuous structure was obtained with a fine dispersion of the minor phase in the matrix. This was also confirmed by the size reduction of PA domains (1.5–0.1 μm), as can be seen in the micrograph of the etched surface [Fig. 15(d)].

PP/PE/PA ternary blend

Figure 16(a) represents the cryofractured surface of the PP/PE/PA ternary blend without the compatibilizer. A very complex structure was obtained, and the lack of adhesion between the components of this system was very well observed: some voids (which could be more likely attributed to PA domains of a spherical shape of about 1.5–2 μm) appeared, and the matrix phase was presented by the polyolefinic compound and was similar to that obtained with the PP/PE blend. The morphology of the etched surface [Fig. 16(b)] of the PP/PE/PA blend also confirmed that PA formed the dispersed phase with spherical droplets of 2 μm.

The morphology of the ternary PP/PE/PA blend with the compatibilizer SEBS-*g*-MAH [Fig. 16(c)] showed a very homogeneous structure with a fine dispersion of PA particles. The etched surface of the same blend had a very homogeneous structure with a uniform dispersion of PA particles in the matrix; a great decrease in the size of the extracted PA domains (0.2–0.5 μm in diameter) was obtained with SEBS-*g*-MAH [see Fig. 16(d)]. These observations explained the effect of the compatibilizer in improving the interfacial adhesion between the dispersed and continuous phases, thus reducing the interfacial tension, and in stabilizing the morphology. All these effects were based on the chemical reaction (Fig. 17) taking place between MAH and the amino end groups of PA,[15] whereas the compatibility between the polyolefinic blends and the compatibilizer was achieved through the affinity of the ethylene–butylene middle blocks of SEBS-*g*-MAH with the polyolefins.

CONCLUSIONS

In this work, the viscoelastic properties of binary and ternary blends of polyolefins and PA6,6 with SEBS and SEBS-*g*-MAH as compatibilizers were investigated in connection with the blend morphologies.

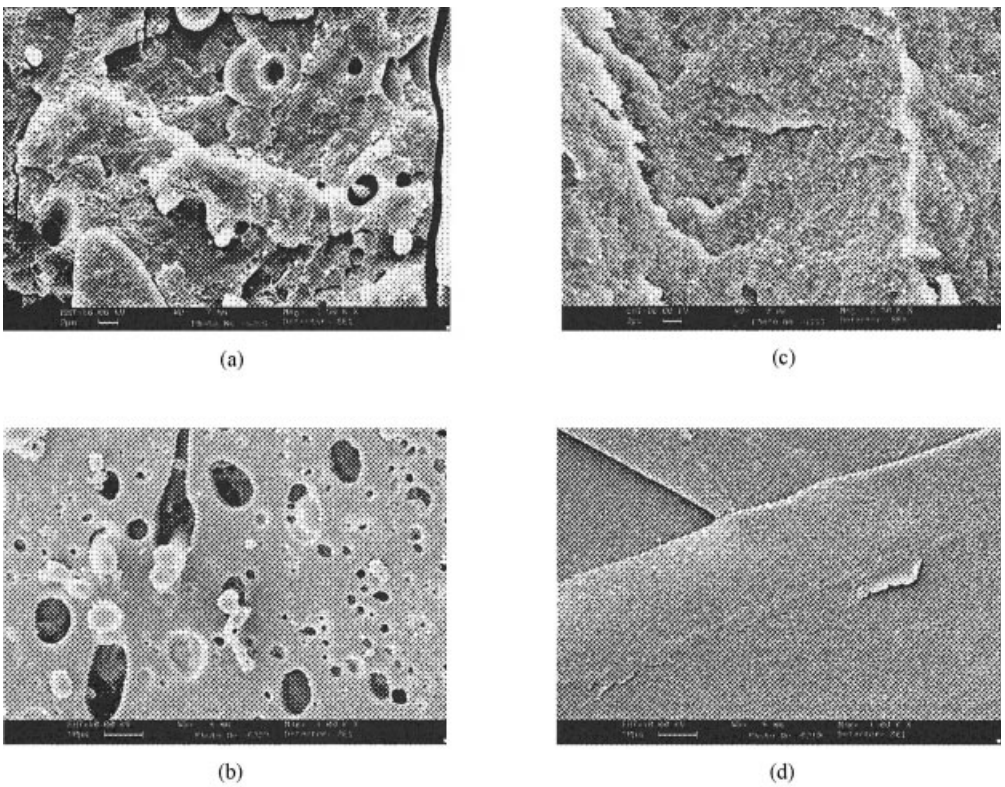

Figure 16 SEM micrographs of (a,c) the cryofractured surface of PP/PE/PA blend samples without and with compatibilizer SEBS-*g*-MAH, respectively, and (b,d) the etched surface of PP/PE/PA blend samples without and with compatibilizer SEBS-*g*-MAH, respectively.

The rheological measurements confirmed the increased interaction between the separate polymers with SEBS-*g*-MAH as a compatibilizer. New covalent bonds might have been formed through an amine–anhydride reaction.

The increases in the complex viscosity for the polyolefinic blends could be attributed to the rubbery nature of SEBS. The transition from a Newtonian flow to a pseudoplastic flow for the blends with the compatibilizer was very pronounced at low frequencies.

G' and G'' for the blends increased as the frequency increased. In the frequency range studied, the high-frequency region was dominated by the G' response; the low-frequency region was dominated by the G'' response, at which terminal relaxation occurred.

A significant change in the morphology of the blends was observed with the addition of the compatibilizer, which led to a fine dispersion with a great reduction in the size of the dispersed second-phase particles.

The cocontinuous structure was also confirmed by rheology, through the increase in the complex viscosity with decreasing frequency, which indicated the presence of the yield stress with the compatibilizer, responsible for the improvement of the interfacial adhesion between the individual phases and the reduction of coalescence.

The authors gratefully acknowledge IPF Dresden (Germany) for the use of its rheometric apparatus and scanning electron microscope. They give special thanks to F. Boehme. The authors also thank A. K. Bledzki of the Institut für Werkstofftechnik at the University of Kassel (Germany) for the use of a twin-screw extruder and an injection machine.

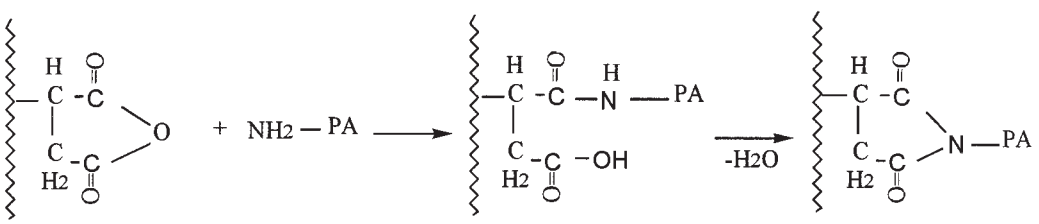

Figure 17 Interfacial reaction between PA6 and compatibilizer SEBS-*g*-MAH.[15]

References

1. Holst-Miettinen, R.; Seppala, J. Polym Eng Sci 1992, 32, 868.
2. Marechal, P.; Coppens, G.; Legras, R.; Dekoninck, J. J Polym Sci Part A: Polym Chem 1995, 33, 757.
3. Xanthos, M.; Dagli, S. S. Polym Eng Sci 1988, 28, 1392.
4. Xanthos, M.; Dagli, S. S. Polym Eng Sci 1991, 31, 929.
5. Rudolf, H. Polym J 1985, 17, 13.
6. Heino, M.; Hietaoja, P.; Seppala, J.; Harmia, T.; Friedrich, K. J Appl Polym Sci 1997, 66, 2209.
7. Vocke, C.; Anttila, U.; Heino, M.; Seppala, J. J Appl Polym Sci 1998, 70, 1923.
8. Fortelny, I.; Krulis, Z.; Michalkova, D.; Horak, Z. Angew Makromol Chem 1999, 270, 28.
9. Ha, C.-S.; Cho, Y.-W.; Go, J.-H.; Cho, W.-J. J Appl Polym Sci 2000, 77, 2777.
10. Stricker, F.; Friedrich, C.; Mulhaupt, R. J Appl Polym Sci 1998, 69, 2499.
11. Mighri, F.; Huneault, M. A.; Ajji, A.; Ko, G. H.; Watanabe, F. J Appl Polym Sci 2001, 82, 2113.
12. Hemmati, M.; Nazodkdast, H.; Panahi, H. S. J Appl Polym Sci 2001, 82, 1129.
13. Paul, D. R.; Barlow, J. W. J Macromol Sci Rev Macromol Chem 1980, 18, 109.
14. Favis, B. D. In Polymer Blends; Paul, D. R.; Bucknall, C. B., Eds.; Wiley: New York, 2000; Vol. 1, p 239.
15. Ohlsson, B.; Tornell, B. Polym Eng Sci 1998, 38, 108.
16. Burgisi, G.; Paternoster, M.; Peduto, N.; Saraceno, A. J Appl Polym Sci 1997, 66, 777.
17. Bassani, A.; Pessan, L. A.; Hage, E. J Appl Polym Sci 2001, 82, 2185.
18. Kelar, K.; Jurkowski, B. Polymer 2000, 3, 1055.
19. Hemmati, M.; Nazodkdast, H.; Panahi, H. S. J Appl Polym Sci 2001, 82, 1138.
20. Pötschke, P.; Paul, D. R. J Macromol Sci 2003, 43, 87.
21. Jafari, S. H.; Pötschke, P.; Stephan, M.; Warth, H.; Alberts, H. Polymer 2002, 43, 6985.
22. Gadekar, R.; Kulkarni, A.; Jogi, J. P. J Appl Polym Sci 1998, 69, 161.
23. Bayram, G.; Yilmazer, U.; Xanthos, M. J Appl Polym Sci 2001, 80, 790.
24. Borve, K. L.; Kotlar, H. K.; Gustafon, C. G. J Appl Polym Sci 2000, 75, 355.
25. Wilhelm, H. M.; Felisberti, M. I. J Appl Polym Sci 2002, 85, 847.
26. Steinmann, S.; Gronski, W.; Friedrich, C. Rheol Acta 2002, 41, 77.
27. Cox, W. P.; Merz, E. H. J Polym Sci 1958, 28, 619.